ResearchGate

See discussions, stats, and author profiles for this publication at: https://www.researchgate.net/publication/224930522

The Participation of 2H-Pyran-2-ones in [4+2] Cycloadditions: An Experimental and Computational Study

ARTICLE *in* EUROPEAN JOURNAL OF ORGANIC CHEMISTRY · OCTOBER 2010

Impact Factor: 3.07 · DOI: 10.1002/ejoc.201000236

CITATIONS
9

READS
14

5 AUTHORS, INCLUDING:

Bogdan Stefane
University of Ljubljana
57 PUBLICATIONS **420** CITATIONS
SEE PROFILE

Andrej Perdih
National Institute of Chemistry
44 PUBLICATIONS **456** CITATIONS
SEE PROFILE

Available from: Andrej Perdih
Retrieved on: 27 January 2016

DOI: 10.1002/ejoc.201000236

The Participation of 2*H*-Pyran-2-ones in [4+2] Cycloadditions: An Experimental and Computational Study

Bogdan Štefane,*[a][‡] Andrej Perdih,[b][‡] Andrej Pevec,[a] Tomaž Šolmajer,[b] and Marijan Kočevar[a]

Keywords: Cycloaddition / Density functional calculations / Donor-acceptor systems / Pyranones / Reaction mechanisms

Experimental and computational DFT studies of the Diels–Alder (DA) reaction mechanism for the series of 2*H*-pyran-2-ones **1** and non-symmetrically substituted alkynes **2**, **10**, and **11** were undertaken. Several 2*H*-pyran-2-ones **1** were treated with *N*,*N*-diethylpropynamine (**2**). The results point toward a polar and asynchronous two-step mechanism that is in line with the characteristics of a polar Diels–Alder (P-DA) reaction mechanism.[5] Unexpected formation of minor products **4a–d** during the reaction of **1** with **2** can be rationalized by considering the easily passable torsion barrier around the newly formed C–C bond that enables two different cyclization modes. The charge transfer (CT) and global reactivity indices analyses demonstrated that in these reactions 2*H*-pyran-2-ones act as electrophiles and *N*,*N*-diethylpropynamine (**2**) acts as a nucleophile reaction partner. The introduction of electron-withdrawing carboxylic substituents on the dienophiles **10** and **11** shifts the DA reaction with 2*H*-pyran-2-ones to a less polar and more synchronous concerted reaction mechanism. Calculated CT as well as values of the global electrophilicity ω and nucleophilicity N indexes revealed that 2*H*-pyran-2-ones act in this case as nucleophiles and reacting dienophiles **10** and **11** as electrophiles. The results are consistent with the experimental data and kinetic analyses, thus providing valuable insights into 2*H*-pyran-2-one chemistry and paving the way for an efficient synthesis of highly functionalized benzene derivatives as well as broadening the mechanistic understanding of these highly versatile reactions.

Introduction

The widely exploited Diels–Alder (DA) reaction represents an important synthetic methodology for the organic chemist. The formation of DA cycloadducts can proceed by different routes. Whereas most of the known reactions proceed according to the rules of orbital symmetry,[1] stepwise reactions involving biradicals,[2] zwitterionic as well as dipolar intermediates[3] are also known. In recent years the boundaries between the concerted and stepwise routes have been intensively investigated.[4,5] For the DA reaction to proceed reasonably fast, an acceptor (A) diene and a donor (D) dienophile (inverse electron-demand reaction scenario) or vice versa (normal electron-demand reaction scenario) substitution pattern is required. Enhanced electrophilicity in the diene and electron-rich substituents on dienophile, however, influence the reaction pathway. This effect could, in general, be described by the frontier molecular orbital (FMO) theory.[1a] Experimental data, however, suggest that the picture is more complex.[6] Moreover, this type of substitution favors an asynchronous concerted mechanism[7] which, in the limit scenario (the stabilization of charges), becomes a stepwise mechanism with a large polar character.[3]

There have been many reports on [4+2] cycloadditions of 2*H*-pyran-2-ones with a variety of dienophiles since they were first described by Alder and Rickert[8] in 1937. The electron-demand of the [4+2] process involving 2*H*-pyran-2-ones as dienes depends highly on the structure of the dienophile. Electron-poor alkenes or alkynes react with 2*H*-pyran-2-ones according to normal electron-demand processes, whereas electron-rich dienophiles tend towards inverse electron-demand cycloadditions. For example, participation of enamines as dienophiles has been described to proceed through an inverse electron-demand cycloaddition,[7f] and cycloadditions involving ynamines are expected to proceed according to the same electron-demand process. A further option is for the reaction to proceed either through a two-stage asynchronous and polar (Michael-type intermediate) or synchronous concerted (Scheme 1, path a) and non-polar transition state

[a] Faculty of Chemistry and Chemical technology, University of Ljubljana
Aškerčeva 5, 1000 Ljubljana, Slovenia
Fax: +386-1-2419 220
E-mail: bogdan.stefane@fkkt.uni-lj.si
[b] National Institute of Chemistry
Hajdrihova 19, 1001 Ljubljana, Slovenia
Fax: +386-1-4760 376
E-mail: andrej.perdih@ki.si
[‡] Bogdan Štefane and Andrej Perdih contributed equally to this work.

Supporting information for this article is available on the WWW under http://dx.doi.org/10.1002/ejoc.201000236.

View this journal online at wileyonlinelibrary.com

© 2010 Wiley-VCH Verlag GmbH & Co. KGaA, Weinheim

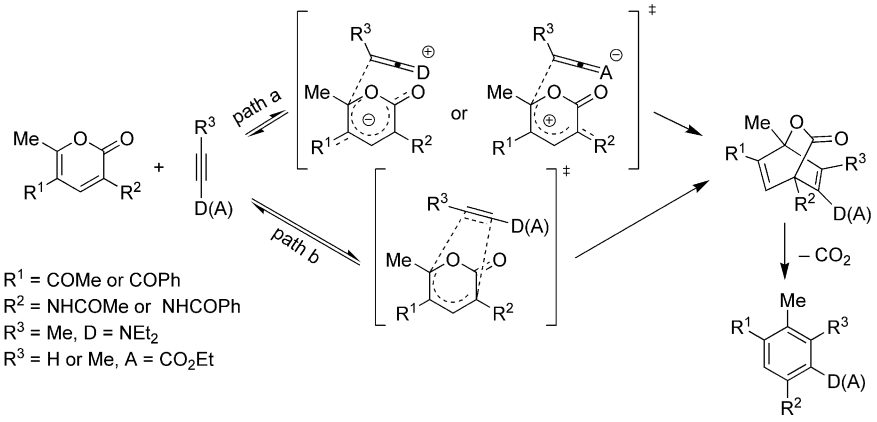

Scheme 1. Mechanistic alternatives for the DA reactions of 2*H*-pyran-2-ones as dienes with the non-symmetrically substituted internal (R^3 = Me, D = NEt_2, or R^3 = Me, A = CO_2Et) and terminal (R^3 = H, A = CO_2Et) alkynes. In the case of a stepwise reaction (path a) a zwitterionic intermediate formed from the electron poor (A substituent) substituted dienophile and the 2*H*-pyran-2-one is also possible.

(Scheme 1, path b),[5] to form the final products after subsequent retro-cycloaddition reaction with the loss of a CO_2 molecule.

More recently, the reactivity indices defined within the conceptual DFT have been widely used to explain the polar Diels–Alder (P-DA) reactions.[5,9] Whereas the global electrophilicity reported by Parr et al.[9a–9d] allows a unique electrophilicity scale[9e] that explains the reactivity in P-DA to be assembled,[5] the local electrophilicity index[9f] allows the regioselectivity in these reactions to be explained through the characterization of the most electrophilic center of the reagents. Recently, Domingo et al. introduced simple global[9g] and local[9h] nucleophilicity indices, which enable an analysis of the behavior of the nucleophilic species.

The purpose of this study was to contribute to a better understanding of the features of the diene (2*H*-pyran-2-one) and dienophile (alkyne derivative) responsible for the concerted or stepwise reaction mechanisms of the DA cycloadditions. Here we report, for the first time, on mechanistic studies of the cycloaddition reactions of *N*,*N*-diethylpropynamine (**2**), ethyl propiolate (**10**), and ethyl but-2-ynoate (**11**) with a series of 2*H*-pyran-2-ones **1**. Such a combination of an electron-rich dienophile (pyruvate enolate) and an electron-deficient diene (5-acetyl-2*H*-pyran-2-ones) can also be found in nature, a manifest example being the biosynthesis of macrophomate.[10] The work of other researchers[11a,11b] and our own experience with 2*H*-pyran-2-ones and their fused derivatives have shown that they are very useful substrates for the DA reaction with alkenes[11a–11h] and alkynes,[11a,11b,11f,11g] leading to the highly regioselective formation of a variety of synthetically interesting precursors, including anilines and *o*-phenylenediamines. Furthermore, it has been shown with two examples that *N*,*N*-diethylpropynamine (**2**) reacts with alkoxycarbonyl-substituted α-pyrones producing non-symmetrically substituted benzene derivatives as single isomers in good yields.[12] The same strategy was adapted by Ireland et al. in their total synthesis of lasalocide A, in which they used the synthetically more useful *N*,*N*-dibenzyl analogue of **2**, and showed that it does not alter the yields of the cycloaddition, producing a highly substituted benzene intermediate with complete regioselectivity.[13] In all the mentioned examples, little attention was paid to the high regioselectivity of the cycloaddition and no mechanistic aspects of these transformations were explored. It was the aim of this study to also provide insights into this area.

Results and Discussion

1. Experimental Study

During our investigation into the DA reactions of 2*H*-pyran-2-one substrates containing a strong electron-donating or electron-deficient substituent at the 5-position, we observed a change in the reaction pathway from the normal to the neutral or the inverse electron-demand scenario.[1c,1e] In due course, the reactions of **1** with *N*,*N*-diethylpropynamine (**2**) (Table 1) were performed in anhydrous tetrahydrofuran (THF) and dichloromethane solutions (by adding *N*,*N*-diethylpropynamine to a stirred solution of **1a**–**d**, ca. 0.20 M) at 25 °C and under an argon atmosphere. The reactions provided [4+2] cycloadducts in all cases. A careful examination of the crude reaction mixtures using ^{1}H NMR spectroscopy showed that there were two products present. The structures of the products **3a**–**d** (as the major products) were confirmed by 2D NMR studies, where the C-3 and C-4 methyl groups (being in the *ortho* position) show strong NOESY correlations. The bicyclic DA intermediates were never observed but were further transformed into the final products **3a**–**d** after the loss of a CO_2 molecule. The co-formed products were determined to be **4a**–**d** (Scheme 2).[14] The formation of the rearranged 2*H*-pyran-2-ones **4a**–**d** attracted our attention and pointed to the possibility of a stepwise mechanism.

Additionally, attempts to perform DA cycloadditions with 2*H*-pyran-2-ones lacking an electron-withdrawing group [such as 3-benzoylamino-5-(4-methoxyphenyl)-2*H*-pyran-2-one and 3-benzoylamino-2*H*-pyran-2-one] at the 5-position were unsuccessful and the corresponding cycloadducts could not be obtained. The fact that *N*,*N*-diethylpro-

 © 2010 Wiley-VCH Verlag GmbH & Co. KGaA, Weinheim

Table 1. [4+2] Cycloadditions of 2*H*-pyran-2-ones **1** with **2**.

	Starting material	R^1	R^2	Solvent	Time [h]	Product [%][a]		
						3	**4**	**3**/**4**[b]
1	**1a**	Me	NHCOMe	CH_2Cl_2	2.5	70	18	3.5:1
2				THF	2.5	68	21	3:1
3				THF/H_2O[c]	2.5	62	18	3:1
4				MeCN	2	47	32	1.5:1
5	**1b**	Ph	NHCOMe	CH_2Cl_2	2.5	51	37	1.2:1
6				THF	2	55	41	1:1
7				THF/H_2O[d]	2	53	42	1:1
8				MeOH	2	30	48	1:1.5
9	**1c**	Me	NHCOPh	CH_2Cl_2	2.5	87[11f]	6	7.5:1
10				THF	2.5	73	21	3:1
11				THF/H_2O[d]	2.5	67	20	3:1
12	**1d**	Ph	NHCOPh	CH_2Cl_2	2.5	71	23	3:1
13				THF	2.5	52	40	1.5:1
14				THF/H_2O[c]	2.5	51	38	1.5:1
15				MeOH	2	29	54	1:2

[a] Average isolated yields after several runs are given. [b] Ratio **3**:**4** determined by ^{1}H NMR analysis of the crude reaction mixture. [c] THF/H_2O = 2:1 (v/v). [d] THF/H_2O = 5:1 (v/v).

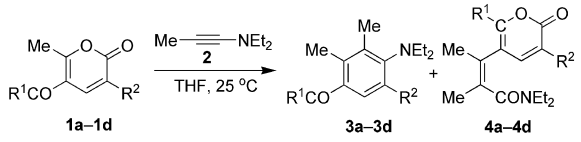

Scheme 2. General reaction of the 2*H*-pyran-2-ones **1a**–**d** with *N*,*N*-diethylpropynamine (**2**).

pynamine (**2**) could be viewed as a nucleophilic reagent is supported, for example, by its ^{13}C NMR signal for the β-carbon atom having a resonance at a higher field (δ = 57.5 ppm) compared with alkylacetylenes (δ = 70–80 ppm),[15] the electron-deficient ethyl propiolate (δ = 74.8 ppm), and ethyl but-2-ynoate (δ = 84.9 ppm). This observation is in agreement with the observation that reagent **2** appears to act as an inverse-electron-demand dienophile in combination with the dienes **1a**–**d**.

Two mechanistic questions result from the formation of the products **3** and **4**: (1) Does the product **3** arise from a concerted or stepwise (in borderline case involving a zwitterionic intermediate) mechanism? (2) Is the formation of the side product **4** a consequence of the relative ease of rotation around the first formed σ C–C bond in the stepwise DA reaction followed by rearrangement of intermediate **7** (see Scheme 4 below for full mechanistic details)? Alternatively, **4** can be formed through intramolecular trapping of the zwitterionic intermediate formed by the initial Michael reaction, which might also be the intermediate in the formation of **3**. Zwitterionic intermediates, which are clear candidates in combinations of A-dienes–D-dienophiles or vice versa have been trapped in a few examples.[3d–3h] However, only Sustmann et al. reported the isolation of zwitterions in a crystalline form.[6] In an effort to gain a better insight into the reaction mechanism, we performed a detailed mechanistic investigation using the substrates **1a**–**c**. When polar intermediates are involved, one would expect a significant solvent effect. However, the solvent polarity was found to have only a moderate effect on the product distribution (the ratio **3a**:**4a** at 29 °C was 3.5:1 in CH_2Cl_2, 3:1 in THF, and 1.5:1 in acetonitrile). Similar observations to ours were previously reported for DA reactions involving polar intermediates.[3g] Additionally, the solvent had only slight influence on the rate constants (the disappearance of **1** following the second-order rate law): for **1a** it is $(1.20 \pm 0.04) \times 10^{-3}$ in toluene, $(4.3 \pm 0.5) \times 10^{-3}$ in acetonitrile, and $(3.2 \pm 0.2) \times 10^{-2}$ L mol^{-1} s^{-1} in dimethyl sulfoxide (DMSO) at 29 °C. We also varied the electronic properties of 2*H*-pyran-2-ones by altering the substituent at the 5-position from acetyl to benzoyl (e.g., **1b**). Due to the low solubility of the substrate **1b** in THF and MeCN, the kinetic measurements for **1b** were performed in $CHCl_3$ and DMSO at 29 °C. The reaction of **1b** with **2** is of a magnitude of 1.5 faster in DMSO $[(9.1 \pm 0.2) \times 10^{-3}]$ than in $CHCl_3$ $[(5.9 \pm 0.2) \times 10^{-3}]$. Thus, the obtained kinetic data suggest a moderate overall influence of the solvent on the rates of the reaction.[1c] In contrast, when zwitterion formation seems to operate, acceleration effects of several powers of ten were observed, for instance in cases of [2+2] cycloaddition, if the polarity of the solvent is increased.[16,3a] However, in our case, the observed influence of the solvent on the kinetics of the reaction cannot rule out a zwitterion mechanism. Recent observations by Harrity and Gomez-Bengoa et al. on the cycloaddition reactions of alkynylboronates support the kinetic results discussed above.[17]

Temperature-dependent measurements were then carried out to determine the activation parameters for the reaction of **1a**–**c** with **2** in toluene and $CHCl_3$. The corresponding Eyring parameters are listed in Table 2.[14] In comparison with substrate **1a**, a slightly lower activation enthalpy for the substrate **1b** was observed, together with a slightly more ordered rate-determining transition state (entry 2, Table 2). Switching of the benzoyl and acetyl moieties at positions 3 and 5 of 2*H*-pyran-2-one (substrates **1b** and **1c**, Table 2) did not have a major influence on the activation parameters. The relatively high negative value of the activation entropy, which is, however, close to the negative values observed in the concerted cycloadditions, does not necessarily rule out the involvement of a zwitterionic species. Namely, similar values have also been observed for transition states with high-polarity.[18]

We turned, therefore, to trapping experiments to check the multi-step nature of the reaction. Despite many attempts, we were not able to trap the putative zwitterionic intermediate using methanol as a solvent. Furthermore, the reaction of **1b** with **2** in the presence of either TMSCl (15 fold excess) or a combination of TMSCl and $(n\text{Bu})_4\text{NN}_3$ (15 fold excess) in anhydrous THF did not give any detectable side products that would indicate the formation of putative zwitterions. When applying water as a co-solvent in THF (1:2, v/v), there was no change in the ratio of the products **3**:**4** formed (Scheme 1). If water were to participate in the reaction as a nucleophile it could be incorporated into the product through a stepwise reaction mechanism according to Scheme 3. When the experiment was conducted with $H_2{}^{18}O$/THF (1:2, v/v), under the same reaction

 © 2010 Wiley-VCH Verlag GmbH & Co. KGaA, Weinheim

Table 2. Activation parameters for the reaction of **1a**–**1c** with *N*,*N*-diethylpropynamine (**2**) and **1c** and **1d** with ethyl propiolate (**10**).

Reaction	R^1	R^2	Solvent	$\Delta H^{\ddagger}$ [kcal mol^{-1}]	$\Delta S^{\ddagger}$ [cal mol^{-1} K^{-1}]	$\Delta G^{\ddagger}$ [kcal mol^{-1}]
1a + **2**	Me	NHCOMe	toluene	11.8 ± 0.4	–34.0 ± 1.4	22.0 ± 1.4
1b + **2**	Ph	NHCOMe	$CHCl_3$	9.8 ± 0.4	–36.0 ± 1.2	20.6 ± 1.2
1c + **2**	Me	NHCOPh	toluene	10.6 ± 0.3	–35.5 ± 0.9	21.2 ± 1.0
1c + **10**	Me	NHCOPh	tetralin	13.8 ± 0.2	–45.3 ± 0.6	27.3 ± 0.6
1d + **10**	Ph	NHCOPh	tetralin	17.9 ± 0.6	–34.4 ± 1.2	28.2 ± 1.3

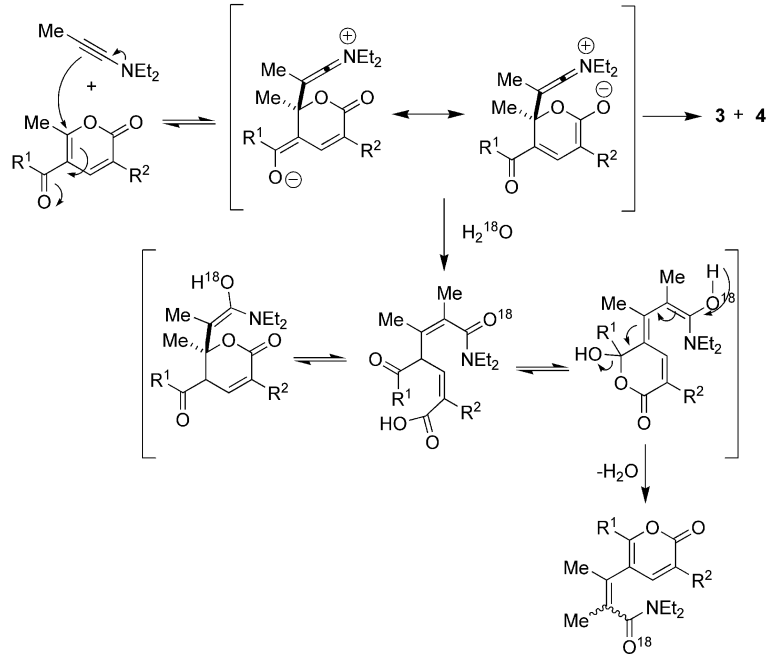

Scheme 3. Possible reaction pathway for $H_2{}^{18}O$ incorporation in the stepwise reaction mechanism of **1** and **2**.

conditions, no products incorporating ^{18}O (as indicated by MS spectroscopy) as a result of external water trapping of the putative zwitterionic intermediate were observed.

The stereochemistry of the double bond in the products **4** was determined by X-ray[14] analyses and a NOESY experiment to be *cis* in all cases. It appears that the configuration of the double bond in the products **4a**–**d** probably originates from the bicyclic intermediate **7**, which is derived from the competing reaction pathway B presented in Scheme 4, followed by a subsequent rearrangement reaction.

Subsequently, we further examined the influence of a change in the electronic properties of the acetylene dienophile. To this end, the reactivity of ethyl propiolate (**10**) and ethyl but-2-ynoate (**11**) dienophiles with 2*H*-pyran-2-one **1c**–**g** was studied (Scheme 5). The reaction of **1c**–**g** with the electron-deficient ethyl propiolate (**10**) was highly regioselective and required harsh reaction conditions, such as heating at 180 °C (heating to reflux in decalin) for several hours, to derive the trisubstituted benzene derivatives **12c**–**g** in good yields[11f,11g] (Table 3). It was shown by Afarinkia et al. that 3- and 5-halo-2*H*-pyran-2-ones react with electron-rich, electron-deficient and also electron-neutral alkenes in a very regio- and stereoselective way, whereas 4-halo derivatives behave completely differently.[19] The 5-(4-methoxyphenyl)-substituted 2*H*-pyran-2-one (**1e**) proved to be the most reactive substrate in combination with alkyne **10**, whereas the 5-acetyl-substituted analogues were found to be the least reactive. To our surprise, we found that a slight change in the structure of the alkyne appears to significantly alter the reactivity. The reaction of **1c**–**g** with ethyl but-2-ynoate (**11**) was anticipated. Interestingly, when the reaction was performed under the same conditions used for the reaction of ethyl propiolate (**10**) or under harsher reaction conditions (200–230 °C in tetralin in a sealed tube), no expected product was formed in the case of **1c**, **1d**, and **1f** even after prolonged heating (for up to 96 h) of the reaction mixture. Instead, the starting material, contaminated with some degradation products, was isolated. On the other hand, the reaction of **1e** and **1g** with **11** was productive after prolonged heating of the reaction mixture with six equivalents of alkyne at 200 °C,[14] resulting in non-regioselective product formation. As shown in Scheme 5, the cycloaddition of **1e** and **1g** gave the regioisomers **13e**, **14e** and **13g**, **14g**. According to ^1H NMR analysis of the crude reaction mixture, the ratios of the regioisomers were **13e**:**14e**, 3:1 and **13g**:**14g**, 5:1, respectively.

To rationalize the observed reactivity of **1** (Scheme 5), we studied the kinetics of the high-temperature reaction of 2*H*-pyran-2-one **1c** and **1d** with ethyl propiolate (**10**). The reac-

 © 2010 Wiley-VCH Verlag GmbH & Co. KGaA, Weinheim

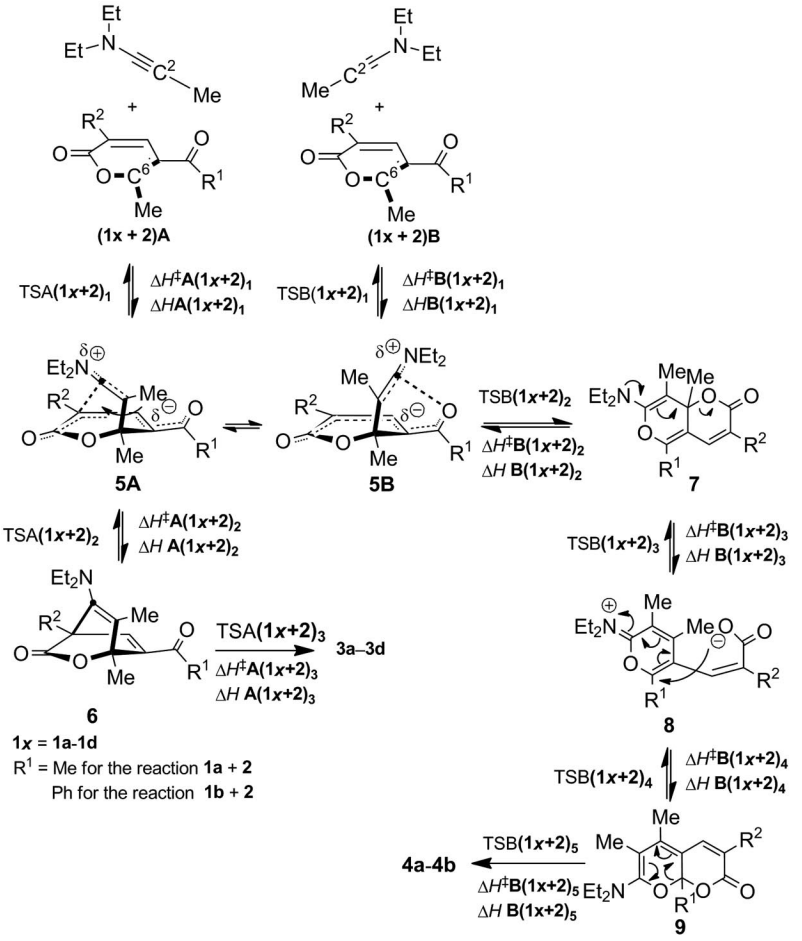

Scheme 4. Pathways for the reaction of 2*H*-pyran-2-ones **1a**–**d** with *N*,*N*-diethylpropynamine (**2**) with defined reaction energies. Path A leads to the main product and path B leads to the side reaction product.

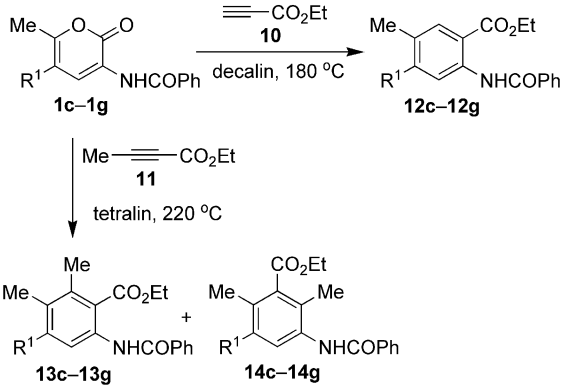

Scheme 5. DA reaction of 2*H*-pyran-2-ones **1c** and **1d** with ethyl propiolate (**10**) and ethyl but-2-ynoate (**11**) dienophiles at high temperature. The reaction of **1g** with **10** was performed in a sealed tube in tetralin at 220 °C for 48 h.

tion could be simply followed by ^{1}H NMR spectroscopic analysis of the crude samples. The experiments were conducted under pseudo-first-order reaction conditions across a temperature range of 130–180 °C in tetralin. The kinetics indicated that the reaction was pseudo-first-order with respect to ethyl propiolate (**10**) under these conditions. An

Table 3. [4+2] Cycloaddition of 2*H*-pyran-2-ones **1c**–**g** with **10** and **11**.

Starting material **1**	Product **12** yield (%)	Product **13** yield (%)	Product **14** yield (%)
1c (R^1 = COMe)	**12c** (94)	**13c** (n.r.)[a]	**14c** (n.r.)[a]
1d (R^1 = COPh)	**12d** (66)	**13d** (n.r.)[a]	**14d** (n.r.)[a]
1e (R^1 = 4-MeOC$_6$H$_4$)	**12e** (75)	**13e** (44)	**14e** (17)
1f (R^1 = CO_2Et)	**12f** (82)	**13f** (n.r.)[a]	**14f** (n.r.)[a]
1g (R^1 = H)	**12g** (44)	**13g** (46)	**14g** (9)

[a] n.r.: no reaction.

Eyring plot[14] allowed us to establish a $\Delta S^{\ddagger}$ value of -45.3 ± 0.6 cal mol^{-1} K^{-1} (Table 2, reaction **1c** + **10**), which is consistent with a highly ordered rate-determining transition state, suggesting a concerted 2*H*-pyran-2-one cycloaddition reaction with alkynes and the absence of intermediates **5a** presumed in the previous reactions involving the formation of a single σ C–C bond. A significantly less negative entropy value ($\Delta S^{\ddagger} = -34.8 \pm 1.2$ cal mol^{-1} K^{-1}, Table 2 and the Supporting Information) was observed for the analog **1d**. The fact that the acetyl group presents less steric hindrance for the transition state compared with the benzoyl moiety in **1d** is manifested in the larger enthalpy ($\Delta H^{\ddagger}$ = 17.9 ± 0.6 kcal/mol) of the rate-determining transition

 © 2010 Wiley-VCH Verlag GmbH & Co. KGaA, Weinheim

state of **1d** (Table 2). Both possible regioisomeric pathways (A and B) for the reaction of 2*H*-pyran-2-ones **1a**–**d** with ethyl propiolate (**10**) and ethyl but-2-ynoate (**11**) are presented in Scheme 6. To provide some insight into the observed experimental results and to complement these findings, we then turned to computational studies.

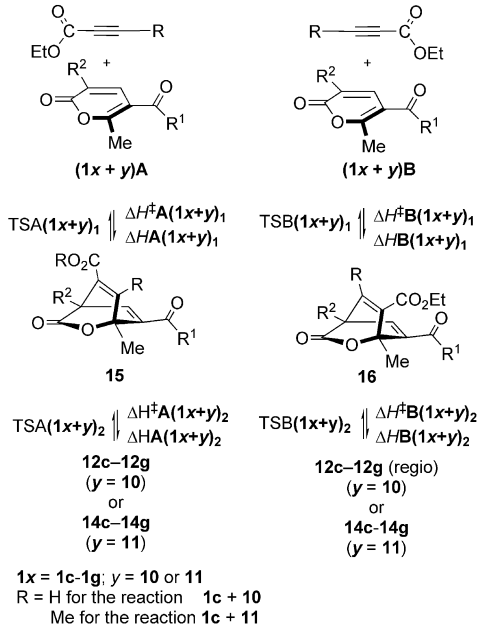

Scheme 6. Pathways for the reaction of 2*H*-pyran-2-ones **1c**–**g** with ethyl propiolate (**10**) and ethyl but-2-ynoate (**11**) (Path A and Path B, two regioisomeric possibilities) with defined reaction energies. For the reaction of **1c**–**e** with **10**, no regioisomeric alternative products **12c**–**g** (regio) were isolated.

2. Computational Study

To support the experimental results and to gain insights into the molecular mechanism of the [4+2] cycloaddition reactions at the atomic level, a computational study of the reactions between the dienes **1a**–**c** and the non-symmetrically substituted dienophiles **2**, **10**, and **11** was performed. Previous theoretical studies on cycloadditions indicated that the geometrical properties as well as the activation energies were in good agreement with the experimental activation energy values if the B3LYP hybrid functional[20] at the density functional level of theory (DFT) was used for the calculation.[21] Since it was expected that a negative charge could be localized on the stationary points, the 6-31+G(d) basis set was used because of its superior ability to accommodate negative charges.[22] The geometry optimizations for the reactants, intermediates, and transition states were performed using the Gaussian03 program[23] and the Berny analytical gradient optimization method. The coordinates of B3LYP 6-31+G(d)-optimized structures are available in the Supporting Information. The optimized stationary points were characterized by frequency calculations to ensure that the minima had zero imaginary frequencies and that the transition states had one imaginary frequency. The zero-point energy (ZPE) corrections were computed at the corresponding DFT level of theory. The intrinsic reaction coordinate (IRC) paths were evaluated to examine the energy changes of the intermediates, the transition states, and the products of the reactions. The energies (enthalpies at 0 K) were determined relative to their optimized reaction complex including the ZPE corrections:

$$\Delta H = \Delta E + \Delta ZPE \quad (1)$$

Because it is possible that the optimized reaction complexes do not fully relate to the minima on the potential energy surface, a careful examination of the optimized complexes was performed. In all cases, the obtained complexes were stable and converged to the optimized geometry. Furthermore, differences in the relative energy were also determined by taking the sum of both reactants as a starting point. It was established that complex formation lowered the relative energies by approximately 1 kcal/mol for the reactions of **1a**+**2** and **1b**+**2**, and by approximately 6 kcal/mol for the reactions **1c**+**10** and **1d**+**11** compared to the sum of energies of the reactants (see Figure S3 of the Supporting Information). Solvent effects were considered by B3LYP/6-31+G(d) single-point calculations of previously obtained gas-phase stationary points at 298 K using a self-consistent reaction field (SCRF) based on the polarizable continuum model of Tomasi et al.[24] The experimental solvents used in kinetic studies: toluene (also used as an approximation for tetralin), chloroform, and dimethyl sulfoxide (DMSO), were modeled by the use of dielectric constants ε = 2.4, 4.9, and 46.7, respectively.

The amount of charge transfer (CT) at the optimized transition state structures was determined by using natural population analysis. Additionally, reactivity indices were computed to understand the reactivity of the molecules in their ground state. These indices were introduced within the DFT framework by Parr et al. and Pearson et al.[9] The electronic chemical potential (μ) describes the changes in the electronic energy with respect to the number of electrons; the chemical hardness (η) and the global electrophilicity (ω), measure the stabilization in the energy when the system acquires an additional electronic charge from the environment. Recently, Domingo et al. introduced a nucleophilicity index (N), which allows the behavior of the nucleophilic species to be assessed.[9] The N-scale is the negative value of the ionization potential calculated by Koopmans' theorem with an arbitrary shifting of the origin. Equations defining these indices are available in the Supporting Information.

2.1. Reaction Energies and Analysis of the Optimized Geometries

Figure 1 depicts the energy profile diagram for the reaction of 2*H*-pyran-2-one **1a** with *N*,*N*-diethylpropynamine (**2**). The enthalpy differences are summarized in Table 4. An analysis of the stationary points obtained for this cycloaddition can be summarized as follows: the rate-determining step of the reaction corresponds to nucleophilic attack of the C-2 of the alkyne on the electrophilic center at C-6 of

 © 2010 Wiley-VCH Verlag GmbH & Co. KGaA, Weinheim

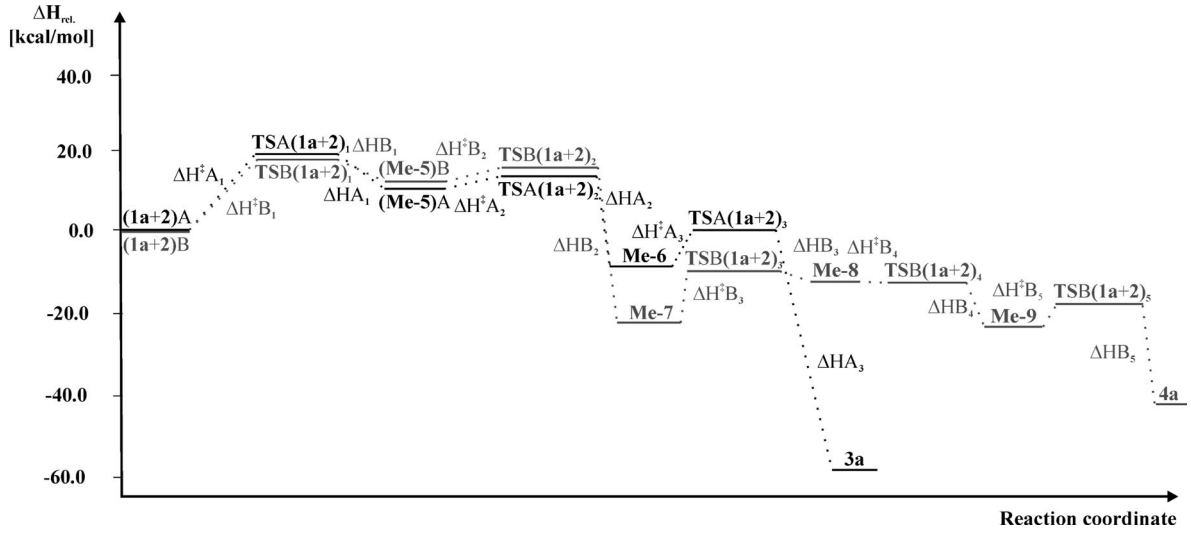

Figure 1. Schematic representation of the reaction coordinate for the cycloaddition of 2*H*-pyran-2-one **1a** to *N*,*N*-diethylpropynamine (**2**). Path A is depicted in black and path B in gray. The depicted values of Δ*H*A and Δ*H*B correspond to the reaction enthalpies Δ*H***A(1a+2)** and Δ*H***B(1a+2)** presented in Table 4.

the diene, affording the reaction intermediates **(Me-5)A** and **(Me-5)B** by passing through the corresponding transition states **TSA(1a+2)$_1$** and **TSB(1a+2)$_1$**. The calculated potential energy barriers associated with these transition states are located at Δ*H*‡**A(1a+2)$_1$** = 19.0 kcal/mol and Δ*H*‡**B(1a+2)$_1$** = 17.1 kcal/mol, respectively. Two possible positions of the dienophile **2** relative to the diene **1a** (geometry A and B in Scheme 4) were investigated to better model the second cyclization step of the reaction yielding either **Me-6** (path A, main product **3a** formation) or **Me-7** (path B, side product **4a** formation) chemical species.

Table 4. Calculated relative energies for the stationary points of the cycloaddition of 2*H*-pyran-2-one **1a** and *N*,*N*-diethylpropynamine (**2**).[a]

	Δ*H*$_{rel.}$ [kcal/mol]*		Δ*H*$_{rel.}$ [kcal/mol]
Δ*H*‡**A(1a+2)$_1$**	19.0	Δ*H*‡**B(1a+2)$_1$**	17.1
Δ*H***A(1a+2)$_1$**	12.3	Δ*H***B(1a+2)$_1$**	13.2
Δ*H*‡**A(1a+2)$_2$**	13.9	Δ*H*‡**B(1a+2)$_2$**	15.2
Δ*H***A(1a+2)$_2$**	–8.2	Δ*H***B(1a+2)$_2$**	–22.0
Δ*H*‡**A(1a+2)$_3$**	–0.3	Δ*H*‡**B(1a+2)$_3$**	–10.6
Δ*H***A(1a+2)$_3$**	–58.7	Δ*H***B(1a+2)$_3$**	–12.1
		Δ*H*‡**B(1a+2)$_4$**	–12.1
		Δ*H***B(1a+2)$_4$**	–26.7
		Δ*H*‡**B(1a+2)$_5$**	–17.0
		Δ*H***B(1a+2)$_5$**	–41.5

[a] All energies were calculated at the B3LYP/6-31+G(d) level, with zero point energy corrections.[4a,25]

The B3LYP/6-31+G(d)-optimized geometries of the transition states **TSA(1a+2)$_1$** and **TSB(1a+2)$_1$** are depicted in Figure 2. The level of synchronicity was measured by the difference in the length of the two σ-bonds formed during the cyclization process. The difference between the bond-forming lengths in **TSA(1a+2)$_1$** (1.9 Å) and **TSB(1a+2)$_1$** (1.5 Å) arises from the highly asynchronous cycloaddition reaction.[4a,21]

The conformational behavior of the intermediates **(Me-5)A** and **(Me-5)B** was further investigated by constructing the torsion potential for the rotation about the newly formed σ C–C bond (Figure 3 and Scheme 4). The atoms labeled 1–4 define the torsion angle. The computed conformational dependence for a rotation about the newly formed C–C bond is presented in Figure 3 (conformations at 15, 30, 45, and 60°). The intermediates **(Me-5)A** (99.57°) and **(Me-5)B** (5.27°) (Scheme 4) are separated by a small rotational energy barrier, indicating that these two conformational states can easily equilibrate before proceeding to the next cyclization step (see Table S5 of the Supporting Information for exact energy values).

Following formation of the first σ C–C bond, the second cyclization step proceeds via the transition states **TSA(1a+2)$_2$** and **TSB(1a+2)$_2$**, resulting in the intermediate compounds **Me-6** and **Me-7**. The obtained values for the unique imaginary frequencies suggest a very flat potential energy surface around the transition state structures and the low calculated activation barriers correlate nicely with analogous ring-closing transitions studied previously.[25] We cannot exclude the possibility that the low imaginary frequency is associated with rotation of one of the methyl groups. The resulting energy barrier of the transition structure Δ*H*‡**B(1a+2)$_2$** is 1.3 kcal/mol higher than the barrier to Δ*H*‡**A(1a+2)$_2$**, indicating the favorable cyclization step of the latter, yielding the **Me-6** reaction intermediate. The experimentally determined product distribution of the final products **3a**:**4a** was 3.5:1 (Table 1); the calculated barrier thus corresponded nicely to a theoretical value of approximately 0.8 kcal/mol. Nevertheless, a caveat should be added that for a precise evaluation of product distribution, higher levels of quantum theory would be necessary. The transition state **TSA(1a+2)$_3$** is associated with the loss of a CO_2 molecule, which ultimately affords the main product **3a**. This

 © 2010 Wiley-VCH Verlag GmbH & Co. KGaA, Weinheim

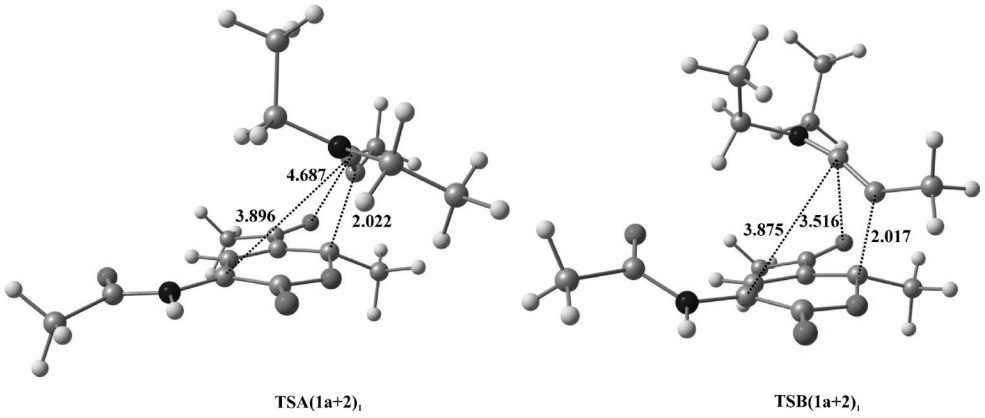

Figure 2. Optimized transition state structures **TSA(1a+2)$_1$** and **TSB(1a+2)$_1$** for the first step of the Diels–Alder reaction of 2*H*-pyran-2-one **1a** and *N*,*N*-diethylpropynamine (**2**). The values of the lengths of the bonds directly involved in the reaction were obtained at the B3LYP/6-31+G(d) level and are given in Ångstrøms [Å]. Two geometries (path A and path B) leading to the reaction products **3a** and **4a**, respectively, were considered.

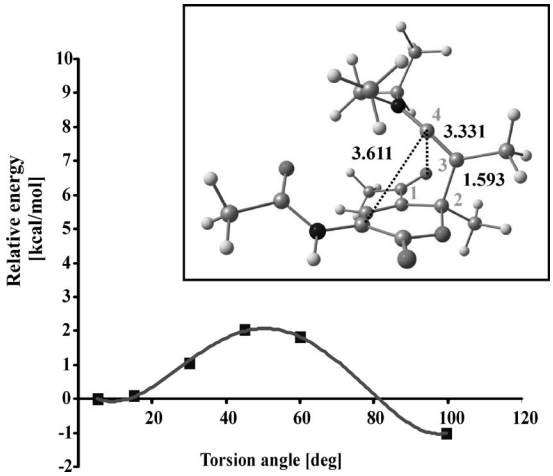

Figure 3. Cycloaddition of 2*H*-pyran-2-one **1a** and *N*,*N*-diethylpropynamine (**2**). The intermediates **(Me-5)B** and **(Me-5)A** (boundary structures) and the computed torsional potential for the rotation (in steps of 15°) about the newly formed σ C–C bond in the intermediate is shown (Scheme 4). The atoms labeled 1–4 define the torsion angle. The geometry of the intermediate structure at a torsion angle of 45° is shown. The relative energy values were scaled from the value at torsion potential of 5.27°. This torsion angle corresponds to the **(Me-5)B** intermediate.

reaction was found to be a very exothermic process, with an energy change of –58.7 kcal/mol compared to the initial reaction complex. The rearrangement leading to the side product **4a** begins with the ring-opening of the **Me-7** pyranone moiety [**TSB(1a+2)$_3$** transition state], yielding the intermediate **Me-8** (Scheme 4 and Table 4). Subsequently, the formation of the side product **4a** proceeds in two steps: In the first step a new bond is formed between the **Me-8** carboxylic oxygen and a carbon atom adjacent to the oxygen of the pyran moiety [**TSB(1a+2)$_4$** transition state] giving a new bicyclic **Me-9** structure. Finally, after ring-opening of the **Me-9** pyran ring [**TSB(1a+2)$_5$** transition state, see Scheme 4] the side product **4a** is obtained, which was found to be 41.5 kcal/mol lower on the energy scale compared with the starting reaction complex.

The cycloaddition of 2*H*-pyran-2-one **1b** and *N*,*N*-diethylpropynamine (**2**) (Table 5) was computationally investigated up to the formation of the second σ C–C bond, affording **Ph-6** and **Ph-7**, because in the **1a**+**2** cycloaddition the initial reaction steps were found to be rate-determining. As in the case of **1a**+**2**, two possible positions of the dienophile **2** relative to the diene **1b** were investigated: Path A, which ultimately leads to the main reaction product **3b**, and Path B, which affords the side product **4b**. The reaction energy profile of the phenyl-substituted compounds is available as Figure S4 of the Supporting Information. The enthalpy change $\Delta H^{\ddagger}$**B(1b+2)$_1$**, which is associated with formation of the transition state structure **TSB(1b+2)$_1$**, was calculated to possess a 0.9 kcal/mol lower relative potential energy barrier [$\Delta H^{\ddagger}$**B(1b+2)$_1$** = 17.0 kcal/mol] than its counterpart transition state structure **TSA(1b+2)$_1$**. In Figure 4, B3LYP/6-31+G(d)-optimized geometries of the transition states **TSA(1b+2)$_1$** and **TSB(1b+2)$_1$** are depicted. The bond lengths in the first transition state once more show a high level of asynchronicity in this DA cycloaddition reaction.[4a,21] The lengths of the forming bonds for the two possible transition state geometries were about 1.7 Å and 1.4 Å. The intermediates **(Ph-5)A** and **(Ph-5)B** are energetically separated by a small barrier of 0.2 kcal/mol. The energy barrier associated with the transition structure **TSB(1b+2)$_2$** is 2.1 kcal/mol higher than that calculated for

Table 5. Calculated relative energies of the cycloaddition of Ph-2*H*-pyran-2-one (**1b**) and *N*,*N*-diethylpropynamine (**2**).[a]

(A)	$\Delta H_{rel.}$ [kcal/mol]	(B)	$\Delta H_{rel.}$ [kcal/mol]
$\Delta H^{\ddagger}$**A(1b+2)$_1$**	17.9	$\Delta H^{\ddagger}$**B(1b+2)$_1$**	17.0
ΔH**A(1b+2)$_1$**	11.8	ΔH**B(1b+2)$_1$**	12.2
$\Delta H^{\ddagger}$**A(1b+2)$_2$**	11.8	$\Delta H^{\ddagger}$**B(1b+2)$_2$**[b]	13.9
ΔH**A(1b+2)$_2$**	–9.4	ΔH**B(1b+2)$_2$**	–22.3

[a] All energies were calculated at the B3LYP/6-31+G(d) level with zero point energy corrections.[4a,25] [b] All attempts to locate the ring-closing transition structure proceeding from the intermediate **(Ph-5)B** were unsuccessful, thus this energy is approximated with the optimized **TSB(1b+2)$_2$** structure with no imaginary frequency.[25]

 © 2010 Wiley-VCH Verlag GmbH & Co. KGaA, Weinheim

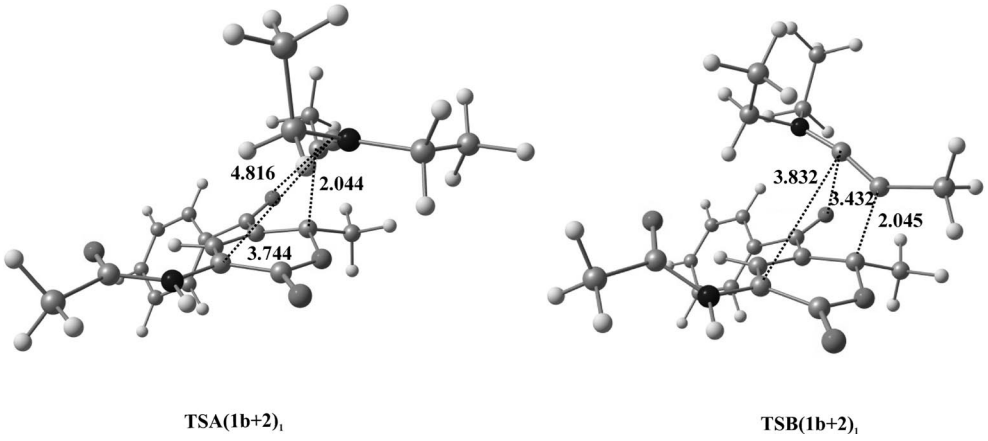

Figure 4. Optimized transition state structures **TSA(1b+2)$_1$** and **TSB(1b+2)$_1$** for the DA reaction of 2*H*-pyran-2-one (**1b**) and *N*,*N*-diethylpropynamine (**2**). The lengths of the bonds directly involved in the reaction obtained at the B3LYP/6-31+G(d) level in toluene are given in angstroms [Å]. Two conformations (Paths A and B) leading to the reaction products **3b** and **4b**, respectively, were considered.

TSA(1b+2)$_2$, indicating (as in the previous case of **1a+2**) that the DA reaction favors the cyclization step leading to formation of the main product. This is in line with the obtained experimental product ratio **3b**:**4b** of 1.2:1 (Table 1).

Investigations into the reaction of 2*H*-pyran-2-one derivative **1c** with ethyl propiolate (**10**) and ethyl but-2-ynoate (**11**) provided two transition state structures that were significantly different from the transition states discussed above. The optimized geometries of the transition states as well as their regioisomeric counterparts are depicted in Figure 5. It can be readily observed that the calculated difference in the partial bond lengths is only 0.79 Å for the transition state **TSA(1c+10)** for the reaction of diene **1c** with **10**. This finding suggests a much higher level of synchronicity, and consequently a much more concerted reaction pathway leading to the formation of the two σ C–C bonds compared to the reactions of **1a+2** and **1b+2** discussed above. The results are consistent with the experimental finding of a large, negative value for the activation entropy (-45.3 ± 0.6 cal mol^{-1} K^{-1}) for the reaction pair **1c+10**. A similar conclusion regarding the synchronicity of the DA reaction can be obtained for the reaction of diene **1c** with ethyl but-2-ynoate (**11**), in which the difference in the bond lengths (Δr) is 0.47 Å. Notably, no intermediate structures

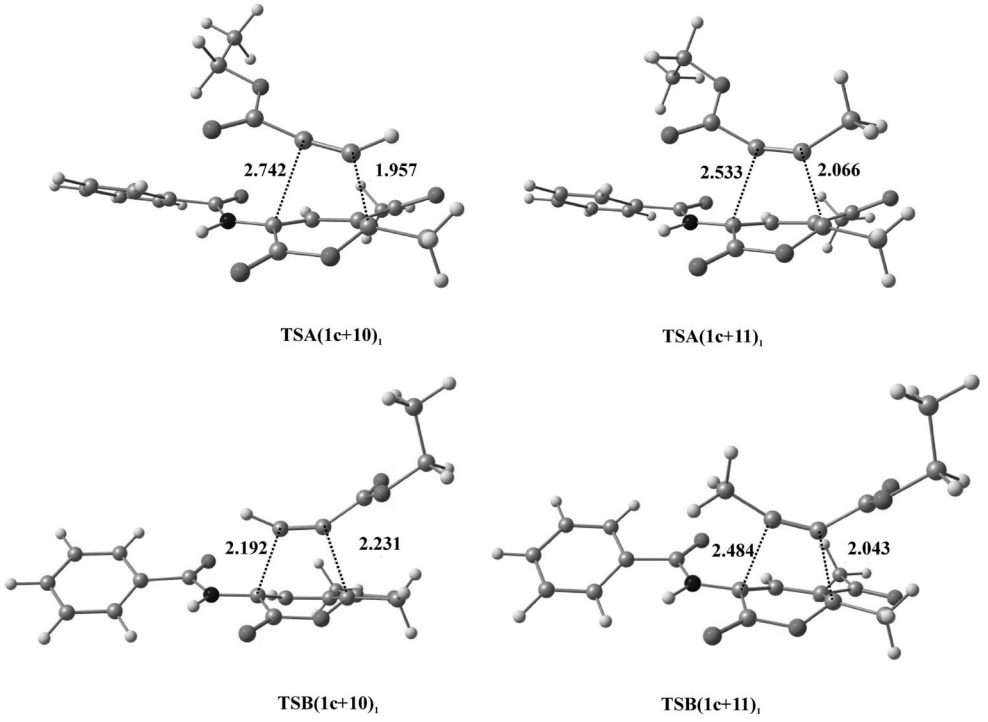

Figure 5. Transition state structures for the reaction of 2*H*-pyran-2-one **1c** with (a) ethyl propiolate (**10**) (left) and (b) ethyl but-2-ynoate (**11**) (right). The lengths of the bonds directly involved in the reaction were obtained at the B3LYP/6-31+G(d) level and are given in angstroms [Å].

 © 2010 Wiley-VCH Verlag GmbH & Co. KGaA, Weinheim

similar to those modeled in the previous reactions with dienophile **2** [e.g., **(Me-5)A**, **(Me-5)B** and **(Ph-5)A**, **(Ph-5)B**] with a single C–C bond formed, could be obtained computationally, which lends support to a highly concerted reaction pathway. The calculated differences in the activation enthalpies for paths A and B in the reactions of **1a** or **1b** with **2** are smaller (by 6–8 kcal/mol) than those calculated for the addition of ethyl propiolate (**10**) and ethyl but-2-ynoate (**11**) to pyranone **1c** (Table 6). This finding is reflected in the harsh experimental reaction conditions and prolonged heating necessary to accomplish product formation in the reactions **1c+10** or **11** compared with the previous reactions. Figure 6 depicts the energy diagram for the reaction of 2*H*-pyran-2-one **1a** with ethyl propiolate (**10**). In terms of the regioselectivity of the **1c+10** reaction, the formation of the **TSA(1c+10)$_1$** is favored over its regioisomer **TSA(1c+10)$_2$** by about 4 kcal/mol. Higher activation enthalpy values (31–33 kcal/mol) were obtained for the reaction of **1c** with **11**. Unfortunately, because all attempts to isolate the product were unsuccessful, the regioselectivity cannot be directly compared to the experimental results for this reaction. However, the lower difference in the activation energy and the fact that pyranones **1e** and **1g** successfully reacted nonregioselectively with **11** after prolonged heating under harsh reactions conditions at 200 °C, renders the reaction of ethyl but-2-ynoate (**11**) with pyranones potentially less regioselective.

Table 6. Calculated relative energies of the cycloaddition between the 2*H*-pyran-2-one **1c** and the ethyl propiolate (**10**) (left) and the ethyl but-2-ynoate (**11**) (right), respectively. (A) and (B) denote two possible orientations of the reactants in the initial complex deriving two regioisomers.[a]

(A)	$\Delta H_{rel.}$ [kcal/mol]		$\Delta H_{rel.}$ [kcal/mol]
$\Delta H^{\ddagger}$**A(1c+10)$_1$**	25.4	$\Delta H^{\ddagger}$**A(1c+11)$_1$**	33.0
ΔH**A(1c+10)$_1$**	–18.0	ΔH**A(1c+11)$_1$**	–8.1
$\Delta H^{\ddagger}$**A(1c+10)$_2$**	–8.8	$\Delta H^{\ddagger}$**A(1c+11)$_2$**	–1.1
ΔH**A(1c+10)$_2$**	–76.5	ΔH**A(1c+11)$_2$**	–61.7
(B)	$\Delta H_{rel.}$ [kcal/mol]		$\Delta H_{rel.}$ [kcal/mol]
$\Delta H^{\ddagger}$**B(1c+10)$_1$**	29.47	$\Delta H^{\ddagger}$**B(1c+11)$_1$**	31.02
ΔH**B(1c+10)$_1$**	–17.91	ΔH**B(1c+11)$_1$**	–10.71
$\Delta H^{\ddagger}$**B(1c+10)$_2$**	–10.16	$\Delta H^{\ddagger}$**B(1c+11)$_2$**	–2.56
ΔH**B(1c+10)$_2$**	–69.75	ΔH**B(1c+11)$_2$**	–58.42

[a] All energies were calculated at the B3LYP/6-31+G(d) level with zero point energy corrections.[4a,25]

In addition to the results of the analysis of the energy changes along the reaction coordinates, the calculated enthalpy differences, corrected by the zero-point energy (ΔH), were supplemented with solvent effects, which were studied by using the polarizable continuum method[24] (Tables S3, S5, S12, and S13 of the Supporting Information). In general, the inclusion of a solvent contribution lowers the free energy of the transition states by 3–5 kcal/mol. This is reasonably close to the values of 2–3 kcal/mol found previously by Domingo et al., in the cycloaddition of 1,3-butadienes with dimethyl acetylenecarboxylate,[21k] and is in line with the limited influence of the solvent on the reaction rates observed experimentally.

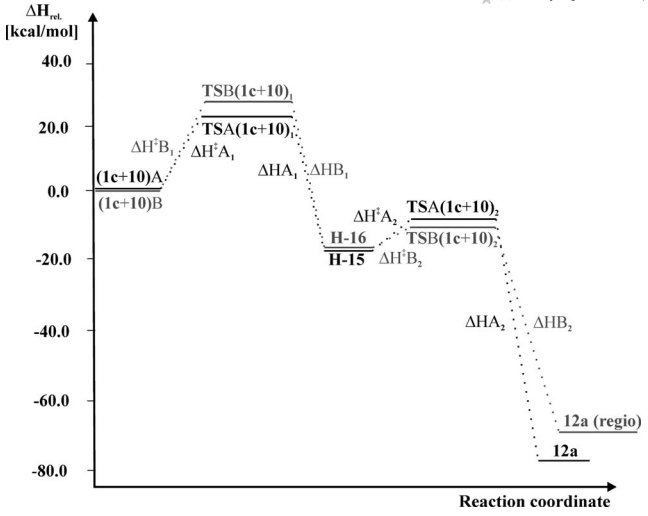

Figure 6. Schematic representation of the reaction coordinate for the cycloaddition of 2*H*-pyran-2-ones **1c** to ethyl propiolate (**10**). Path A is depicted in black and the regioalternative path B in gray. The depicted values of ΔHA and ΔHB correspond to the reaction enthalpies ΔHA(1c+10) and ΔHB(1c+10) presented in Table 6.

2.2. Global Reactivity Indices and Charge-Distribution Analysis

The stationary points of the four studied DA reactions were further analyzed and the amount of charge transfer (CT) at the optimized transition states,[26,27] as well as global reactivity indices defined in the context of the DFT theory,[9] were calculated (see Tables S6–S7 and Tables S14–15 of the Supporting Information). In addition, the nucleophilicity index (N), which allows the behavior of the nucleophilic species to be assessed, was determined.[9] Representative data are presented in Table 7.

The amount of charge transferred during transition state formation was determined by natural population analysis (Tables S8–S11 and S16–19 of the Supporting Information). In the reaction of **1a** with **2**, the values of charge [0.43 au (path A) and 0.45 au (path B)] transferred from **2** to **1a** suggest a polar reaction pathway for the reaction. We would also like to note that the relatively large charge transfer and high non-symmetry of the C–C bond formation in the reaction of **1** with **2** might even support an ionic character for these reactions. As expected, the comparable reaction of **1b+2** showed similar behavior [0.42 au (path A) and 0.44 au (path B)] for the charge transfer from **2** to **1b**. Furthermore, inclusion of solvent effects had only marginal effects on the CT values, thus complementing nicely the observed minor influence of the solvent on the observed rate constants. The large observed CT of 0.42–0.45 au for the neutral species entering the reaction is in line with the P-DA reaction.[5] On the other hand, the values of CT in the reverse direction, from the pyranone **1c** to the substituted carboxylate dienophiles **10** and **11**, are considerably lower (0.05 au and 0.04 au).[5] These values exemplify the significant change in the polar character of the latter adduct.

 © 2010 Wiley-VCH Verlag GmbH & Co. KGaA, Weinheim

Table 7. Global reactivity indices of the reactants[a] involved in the cycloaddition reactions of 2*H*-pyran-2-ones **1a**–**f** with the non-symmetrically substituted alkynes **2**, **10**, and **11**.

Compound	μ [au]	η [au]	ΔN_{max}	ω [eV]	N[b]
Ethyl propiolate (**10**)	−0.1756	0.1509	1.1637	2.78	1.46
2*H*-Pyran-2one (**1b**)	−0.1599	0.1501	1.0653	2.32	3.01
2*H*-Pyran-2one (**1a**)	−0.1606	0.1586	1.0126	2.21	2.88
2*H*-Pyran-2-one (**1c**)	−0.1589	0.1554	1.0221	2.21	2.97
2*H*-Pyran-2-one (**1d**)	−0.1593	0.1470	1.0837	2.35	3.07
2*H*-Pyran-2-one (**1f**)	−0.1561	0.1558	1.0019	2.12	3.04
2*H*-Pyran-2-one (**1g**)	−0.1507	0.1528	0.9862	1.98	3.23
2*H*-Pyran-2-one (**1e**)	−0.1447	0.1455	0.9945	1.96	3.49
Ethyl but-2-ynoate (**11**)	−0.1605	0.2294	0.6997	1.53	1.91
1-(Diethylamino)propyne (**2**)	−0.0952	0.1988	0.4789	0.62	4.11

[a] Global electrophilicity (ω); electronic chemical potential (μ) and chemical hardness (η); ΔN_{max} maximal amount of electronic charge that the electrophile can accept, and the nucleophilicity index (N). [b] The HOMO energy of tetracyanoethylene (TCE) is –0.34577 au at the same level of theory.[9]

The calculated electronic characteristics can also be correlated with the measured, as well as calculated, activation parameters. Reactions with lower CT, for example, reaction of pyranone **1c** with **10**, correlated with the experimentally and computationally observed higher energy barriers necessary for this DA reaction to occur. In contrast, higher CT values for the **1a**+**2** and **1b**+**2** reactions corresponded to a lower activation energy barrier. This also leads to a change in the reaction mechanism and suggests that a significantly more polar reaction takes place in the latter cases.[5]

The electronic chemical potential μ of the dienes **1a**–**d** (–0.1606, –0.1599, –0.1589, and 0.1593 au, respectively) is lower than those of ynamine **2** (–0.0952 au), indicating that CT will take place during cycloaddition from the ynamine **2** to the dienes **1a**–**d**. On the other hand, the electronic chemical potential of the electron-deficient acetylenes **10** (–0.1756 au) is lower than that of the dienes. Thus, for the DA reaction between **10** and the dienes **1c** and **1d**, there is a clear reversal in the flow of the CT going from the dienes to acetylene derivative **10**, which possesses the lowest chemical potential value of the series.

A low value of global electrophilicity (ω = 0.62 eV) for compound **2** classifies this species as a marginal electrophile. On the other hand, a relatively high value of ω calculated for pyranone dienes (ω = 1.96–2,32 eV) puts these chemical species among the moderate electrophiles on the electrophilicity scale for common substrates involved in the DA reactions.[5] In comparison to the electrophilicity of **1a** and **1b**, the difference $\Delta\omega$ = 1.59 eV and 1.7 eV confirms the flow of the electrons from compound **2** to the pyranone, as well as the polar nature of these types of reaction.[5] This can be further correlated with the experimental observation from ^{13}C NMR spectroscopy (see above), which supports the notion that **2** acts as a nucleophile in the reaction with dienes **1a** and **1b**. Similarly, compound **10**, which possesses a greater global electrophilicity index (ω = 2.78 eV) compared with *2H*-pyran-2-ones, results in a reverse flow of electrons during the reaction. The smaller difference with **1c** ($\Delta\omega$ = 0.57 eV) is in accordance with the lower polar character of this DA reaction. In addition, analysis of the nucleophilicity index[9] N showed that it was in line with the previously observed behavior. *N*,*N*-Diethylpropynamine (**2**) has a larger nucleophilic index (N = 4.11 eV) compared with the reacting pyranones **1a**–**d** (N = 2.88–3.07 eV), which renders this species nucleophilic in the polar DA reactions. On the other hand, the reverse situation is observed for the reaction of **1c** (N = 2.97 eV) with compounds **10** (N = 1.46 eV) and **11** (N = 1.97 eV), in which the pyranones act as nucleophiles. Due to the smaller difference in the N index, a less polar character is displayed for the **1c**+**10** reaction.

Conclusions

The molecular mechanisms for [4+2] cycloaddition reactions involving a combination of acetylene derivatives and 2*H*-pyran-2-ones have been studied by a combination of experimental and computational DFT methods. Our theoretical and experimental investigations revealed the polar character of the DA reaction between *N*,*N*-diethylpropynamine (**2**) and 2*H*-pyran-2-ones **1**. These reactions are described by an asynchronous, two-step mechanism characterized by the rate-limiting nucleophilic attack, Michael addition, of the alkyne **2** to the electron-deficient 2*H*-pyran-2-one derivatives **1** with the formation of a C–C bond. This is in line with the characteristics of a P-DA reaction mechanism.[5] Ring closure affords the final cycloadduct through the formation of the second C–C bond in the subsequent stage of the reaction. The higher CT and global reactivity indices confirmed the polar nature of the reaction and identified ynamine **2** as a nucleophilic species in these polar DA reactions. The observed mechanism has parallels in the stepwise mechanism studied by Jorgensen et al. in the enzymatic environment of the macrophomate synthase, where evidence was presented that the Diels–Alder transition state is less stable than the Michael-aldol transition state,[10c] as well as in recent examples of the competition between a polar Diels–Alder and a two-step reaction described by Bongini and Panunzio et al.[28] The unexpected formation of the minor products **4a**–**d** during the reaction of **1** with **2** can be rationalized by considering the low torsion barrier around the newly formed C–C bond, which enables two different cycli-

 © 2010 Wiley-VCH Verlag GmbH & Co. KGaA, Weinheim

zation modes. Singleton et al.[29] have employed a dynamic trajectory approach[30] to point out the possibility of non-statistical recrossing to explain the yield of minor products.

The change in the electrostatic nature of the acetylene derivatives to the carboxyl-substituted chemical species **10** and **11** resulted in a change in the reaction pathway, with 2*H*-pyran-2-ones **1** displaying a more synchronous, concerted pathway. Furthermore, a smaller CT in the reverse direction to the previous reaction, a lower difference in the global electrophilicity ω and nucleophilicity index N, favored a less polar and more energy-demanding reaction pathway. In these DA reactions, 2*H*-pyran-2-ones **1** played the role of the nucleophile. Overall, all the computational results consistently corroborated the available experimental data and kinetic analyses. We believe that the results of this study will assist in the identification of compatible diene–dienophile substrates for use in 2*H*-pyran-2-one chemistry that will enable efficient cycloaddition reactions to be developed and lead to highly functionalized benzene derivatives. The results should also contribute to a deeper mechanistic understanding of these highly versatile reactions.

Experimental Section

General Procedure for the Cycloaddition of 2*H*-Pyran-2-ones 1a–c with *N*,*N*-Diethyl-1-propyn-1-amine: To a solution of one of the 2*H*-pyran-2-ones **1a**–**c** (1 mmol) in THF (5 mL), *N*,*N*-diethylpropynamine (222 mg, 2 mmol) was added. The reaction mixture was stirred at r.t. for 0.75–2.5 h and then evaporated to dryness. Purification of the residue by column chromatography (light petroleum/ethyl acetate, 5:3 then 1:1) gave the products **3a**–**c**. Additionally, **4a**–**c** were isolated as white solids.

***N*-[5-Acetyl-2-(diethylamino)-3,4-dimethylphenyl]acetamide (3a):** Yield 68%; yellow oil. IR (NaCl): $\tilde{\nu}$ = 3318 (br), 2969 (m), 1686 (s), 1574 (s), 1507 (s), 1409 (m), 1322 (m), 1268 (m), 1216 (m), 1188 (m), 888 (w) cm^{-1}. ^{1}H NMR (300 MHz): δ = 1.03 (t, *J* = 7.0 Hz, 6 H, Et), 2.19 (s, 6 H, Me), 2.27 (s, 3 H, Me), 2.57 (s, 3 H, Me), 3.00–3.08 (m, 2 H, Et), 3.15–3.22 (m, 2 H, Et), 8.61 (s, 1 H, Ph), 9.17 (br. s, 1 H, NH) ppm. ^{13}C NMR (75.5 MHz): δ = 14.8, 15.5, 16.1, 24.7, 30.1, 48.3, 115.2, 130.8, 135.7, 137.5, 137.6, 137.9, 167.7, 203.4 ppm. MS (EI, 70 eV): *m*/*z* (%) = 276 (100) [M]$^+$, 261 (50), 247 (55), 205 (90), 189 (53). HRMS: calcd. for $C_{16}H_{24}N_2O_2$: 276.1838; found 276.1845.

***N*-{5-[(1*Z*)-3-(Diethylamino)-1,2-dimethyl-3-oxoprop-1-enyl]-6-methyl-2-oxo-2*H*-pyran-3-yl}acetamide (4a):** Yield 21%; m.p. 169–170 °C (Et_2O/CH_2Cl_2). IR (KBr): $\tilde{\nu}$ = 3328 (br), 2974 (m), 2932 (m), 1681 (s), 1627 (s), 1564 (s), 1518 (s), 1430 (s), 1383 (s), 1327 (m), 1289 (m), 1238 (s), 1167 (m), 1123 (m), 1042 (m), 923 (s), 776 (s) cm^{-1}. ^{1}H NMR (300 MHz): δ = 0.81 (t, *J* = 7.0 Hz, 3 H, Et), 1.10 (t, *J* = 7.0 Hz, 3 H, Et), 1.88 (s, 3 H, Me), 1.94 (s, 3 H, Me), 2.18 (s, 3 H, Me), 2.20 (s, 3 H, Me), 2.66–3.73 (m, 4 H, Et), 7.91 (br. s, 1 H, NH), 8.03 (s 1 H, =CH-) ppm. ^{13}C NMR (75.5 MHz): δ = 12.0, 14.2, 16.2, 17.8, 18.4, 24.4, 37.2, 42.1, 117.8, 122.2, 125.8, 126.9, 133.1, 152.3, 159.6, 169.1, 170.7 ppm. MS (EI): *m*/*z* (%) = 320 (100) [M]$^+$, 205 (88), 177 (40), 100 (42), 72 (43). HRMS: calcd. for $C_{17}H_{24}N_2O_4$: 320.1736; found 320.1745. $C_{17}H_{24}N_2O_4$ (320.39): calcd. C 63.73, H 7.55, N 8.74; found C 63.82, H 7.89, N 8.89.

General Procedure for the Cycloaddition of 2*H*-Pyran-2-ones 1c–g with Ethyl Propiolate (10) and Ethyl But-2-ynoate (11):[11f,11g] A mixture of the starting 2*H*-pyran-2-one **1c**–**g** (2 mmol) and dienophile **10** or **11** (12 mmol) in decaline or tetraline (6 mL) was heated at 160–195 °C for 6–48 h. After the reaction was completed, the volatile material was evaporated under high vacuum and the residue was purified by column chromatography on SiO_2.

Ethyl 2-Benzamido-5-methylbenzoate (12g): After purification by column chromatography (EtOAc/petroleum ether, 1:5 then 1:3), white crystals of **12g** were obtained; yield 180 mg (44%); m.p. 151.5–152.5 °C (CH_2Cl_2/petroleum ether). IR (KBr): $\tilde{\nu}$ = 3445, 1749, 1634, 1515, 1294, 1248, 1090, 989 cm^{-1}. ^{1}H NMR (300 MHz): δ = 1.42 (t, *J* = 7.0 Hz, 3 H, Et), 2.35 (s, 3 H, Me), 4.40 (q, *J* = 7.0 Hz, 2 H, Et), 7.40 (dd, *J* = 8.5, 2.0 Hz, 1 H, Ph), 7.47–7.56 (m, 3 H, Ph), 7.88 (d, *J* = 2.0 Hz, 1 H, Ph), 8.02–8.05 (m, 2 H, Ph), 8.81 (d, *J* = 8.5 Hz, 1 H, NH) ppm. ^{13}C NMR (75.5 MHz): δ = 14.2, 20.7, 61.4, 115.3, 120.4, 127.3, 128.7, 130.9, 131.7, 132,0, 135.0, 135.3, 139.5, 165.4, 168.6 ppm. MS (ES+): *m*/*z* = 284 [M + H]$^+$. HRMS: calcd. for $C_{17}H_{18}NO_3$: 284.1287; found 284.1285. $C_{17}H_{17}NO_3$ (283.33): calcd. C 72.071, H 6.05, N 4.94; found C 71.95, H 6.01, N 5.01.

Ethyl 5-Benzamido-4′-methoxy-2,3-dimethylbiphenyl-4-carboxylate (13e): After purification by column chromatography (EtOAc/petroleum ether, 1:5 then 1:3), white crystals of **13e** were obtained; yield 180 mg (44%); m.p. 151.5–152.5 °C (Et_2O/petroleum ether). IR (KBr): $\tilde{\nu}$ = 3437 (brw), 1724 (s), 1639 (s), 1611 (m), 1512 (s), 1459 (m), 1292 (m), 1246 (s), 1192 (m), 1108 (m), 1039 (s), 831 (s), 692 (s) cm^{-1}. ^{1}H NMR (300 MHz): δ = 1.40 (t, *J* = 7.0 Hz, 3 H, Et), 2.17 (s, 3 H, Me), 2.25 (s, 3 H, Me), 3.83 (s, 3 H, Me), 4.42 (q, *J* = 7.0 Hz, 2 H, Et), 6.91 (AA′XX′, *J* = 8.5 Hz, 2 H, *p*MeOAr), 7.20 (AA′XX′, *J* = 8.5 Hz, 2 H, *p*MeOAr), 7.44–7.56 (m, 3 H, Ph), 7.68 (s, 1 H, Ph), 7.77 (br. s, 1 H, NH), 7.85–7.88 (m, 2 H, Ph) ppm. ^{13}C NMR (75.5 MHz): δ = 14.2, 14.7, 17.3, 55.3, 61.2, 113.5, 126.0, 126.7, 127.1, 128.8, 129.3, 130.4, 131.9, 133.1, 133.4, 134.6, 136.4, 140.7, 158.7, 165.8, 170.1 ppm. MS (ES+): *m*/*z* = 404 [M + H]$^+$. HRMS: calcd. for $C_{25}H_{26}NO_4$: 404.1862; found 404.1866.

Ethyl 5-Benzamido-4′-methoxy-2,4-dimethylbiphenyl-3-carboxylate (14e): After purification by column chromatography (EtOAc/petroleum ether, 1:5 then 1:3), white crystals of **14e** were obtained; yield 70 mg (17%); m.p. 137.5–138.5 °C (Et_2O/petroleum ether). IR (KBr): $\tilde{\nu}$ = 3451 (br., w), 1669 (s), 1579 (s), 1509 (s), 1405 (m), 1283 (s), 1246 (s), 1176 (m), 1138 (m), 836 (m), 697 (m) cm^{-1}. ^{1}H NMR (300 MHz): δ = 1.41 (t, *J* = 7.0 Hz, 3 H, Et), 2.18 (s, 3 H, Me), 2.41 (s, 3 H, Me), 3.85 (s, 3 H, Me), 4.45 (q, *J* = 7.0 Hz, 2 H, Et), 6.94 (AA′XX′, *J* = 8.5 Hz, 2 H, *p*MeOAr), 7.26 (AA′XX′, *J* = 8.5 Hz, 2 H, *p*MeOAr), 7.46–7.56 (m, 3 H, Ph), 7.91–7.93 (m, 2 H, Ph), 8.25 (s, 1 H, Ph), 9.87 (br. s, 1 H, NH) ppm. ^{13}C NMR (75.5 MHz): δ = 14.1, 17.3, 19.0, 55.3, 61.7, 113.5, 121.2, 121.3, 127.1, 128.8, 130.4, 131.1, 131.8, 134.1, 134.4, 134.8, 136.9, 145.3, 158.8, 165.0, 169.8 ppm. MS (ES+): *m*/*z* = 404 [M + H]$^+$. HRMS: calcd. for $C_{25}H_{26}NO_4$: 404.1862; found 404.1866.

Supporting Information (see footnote on the first page of this article): Full experimental data, kinetic details, X-ray structure data and computational details.

Acknowledgments

The Ministry of Higher Education, Science and Technology of the Republic of Slovenia as well as the Slovenian Research Agency (P1-0012, P1-0230-0103, and PS-0175) are gratefully acknowledged for their financial support. G. Miličič, K. Zorko, and K. Slanc, Faculty of Chemistry and Chemical Technology University of Ljubljana,

 © 2010 Wiley-VCH Verlag GmbH & Co. KGaA, Weinheim

are gratefully acknowledged for laboratory assistance, and Dr. Urban Bren from the National Institute of Chemistry is thanked for stimulating discussions in the initial stage of this work.

[1] a) I. Fleming, *Frontier Orbitals and Organic Chemical Reactions*, John Wiley & Sons, New York, **2000**; b) J. Sauer, *Angew. Chem. Int. Ed. Engl.* **1967**, *6*, 17–33; c) J. Sauer, R. Sustmann, *Angew. Chem. Int. Ed. Engl.* **1980**, *19*, 779–807; d) K. H. Houk, J. González, Y. Li, *Acc. Chem. Res.* **1995**, *28*, 81–90; e) E. Eibler, P. Höcht, B. Prantl, H. Roßmaier, H. M. Schuhbauer, H. Wiest, J. Sauer, *Liebigs Ann./Recl.* **1997**, 2471–2484.

[2] a) J. C. Scaiano, V. Wintgens, K. Haider, J. A. Berson, *J. Am. Chem. Soc.* **1989**, *111*, 8732–8733; b) K. Lücking, M. Rese, R. Sustmann, *Liebigs Ann.* **1995**, 1129–1138; c) M. Rese, M. Dern, K. Lücking, R. Sustmann, *Liebigs Ann.* **1995**, 1139–1152; d) G. Orlova, J. D. Goddard, *J. Org. Chem.* **2001**, *66*, 4026–4035; e) K. L. Handoo, Y. Lu, D. V. Parker, *J. Am. Chem. Soc.* **2003**, *125*, 9381–9387.

[3] For reviews on the topic, see: a) R. Huisgen, *Acc. Chem. Res.* **1977**, *10*, 117–124; b) R. Huisgen, *Acc. Chem. Res.* **1977**, *10*, 199–206; c) H. K. Hall, A. B. Padias, *Acc. Chem. Res.* **1990**, *23*, 3–9. For examples, see: d) P. G. Gassman, D. B. Gorman, *J. Am. Chem. Soc.* **1990**, *112*, 8624–8626 and references cited therein; e) F. Jensen, C. S. Foote, *J. Am. Chem. Soc.* **1987**, *109*, 6376–6385; f) K.-P. Hartmann, M. Heuschmann, *Angew. Chem.* **1989**, *101*, 1288–1290; g) R. Sustmann, S. Tappanchai, H. Bandmann, *J. Am. Chem. Soc.* **1996**, *118*, 12555–12561; h) R. Sustmann, M. Rogge, U. Nüchter, H. Bandmann, *Chem. Ber.* **1992**, *125*, 1657–1664.

[4] a) R. Gordillo, K. N. Houk, *J. Am. Chem. Soc.* **2006**, *128*, 3543–3553; b) G. A. Griffith, I. H. Hillier, A. C. Moralee, J. M. Percy, R. Roig, M. A. Vincent, *J. Am. Chem. Soc.* **2006**, *128*, 13130–13141; c) R. G. Iafe, K. N. Houk, *Org. Lett.* **2006**, *8*, 3469–3472; d) L. R. Domingo, M. T. Picher, P. Arroyo, *Eur. J. Org. Chem.* **2006**, 2570–2580; e) L. R. Domingo, *Eur. J. Org. Chem.* **2004**, 4788–4793; f) L. R. Domingo, M. J. Aurell, P. Pérez, R. Contreras, *J. Org. Chem.* **2003**, *68*, 3884–3890.

[5] L. R. Domingo, J. A. Saez, *Org. Biomol. Chem.* **2009**, *7*, 3576–3583.

[6] a) J. Sauer, H. Wist, A. Mielert, *Chem. Ber.* **1964**, *97*, 3183–3207; b) C. Rücker, D. Lang, J. Sauer, H. Friege, R. Sustmann, *Chem. Ber.* **1980**, *113*, 1663–1690; c) R. Sustmann, M. Rogge, U. Nüchter, H. Badmann, *Chem. Ber.* **1992**, *125*, 1646–1656; d) R. Sustmann, M. Rogge, U. Nüchter, J. Harvey, *Chem. Ber.* **1992**, *125*, 1665–1667.

[7] a) R. Sustmann, W. Sicking, *J. Am. Chem. Soc.* **1996**, *118*, 12562–12571; b) W. L. Jorgensen, D. Lim, J. F. Blake, *J. Am. Chem. Soc.* **1993**, *115*, 2936–2942; c) D. M. Birney, K. N. Houk, *J. Am. Chem. Soc.* **1990**, *112*, 4127–4133; d) R. J. Loncharich, F. K. Brown, K. N. Houk, *J. Org. Chem.* **1989**, *54*, 1129–1134; e) K. N. Houk, R. J. Loncharich, J. F. Blake, W. L. Jorgensen, *J. Am. Chem. Soc.* **1989**, *111*, 9172–9176; f) H. L. Gingrich, D. M. Roush, W. A. Van Saun, *J. Org. Chem.* **1983**, *48*, 4869–4873.

[8] K. Alder, H. F. Rickert, *Ber. Dtsch. Chem. Ges.* **1937**, *70*, 1354–1363.

[9] a) R. G. Parr, R. G. Pearson, *J. Am. Chem. Soc.* **1983**, *105*, 7512–7516; b) R. G. Parr, W. Yang, *Density Functional Theory of Atoms and Molecules*, Oxford University Press: New York, **1989**; c) R. G. Parr, L. von Szentpaly, S. Liu, *J. Am. Chem. Soc.* **1999**, *121*, 1922–1924; d) R. G. Pearson, *Chemical Hardness: Applications from Molecules to Solids*, Wiley-VHC, Weinheim, Germany, **1997**; e) L. R. Domingo, M. J. Aurell, P. Perez, R. Contreras, *Tetrahedron* **2002**, *58*, 4417–4423; f) L. R. Domingo, R. Contreras, *J. Phys. Chem. A* **2002**, *106*, 6871–6879; g) L. R. Domingo, E. Chamorro, P. Pérez, *J. Org. Chem.* **2008**, *73*, 4615–4624; h) P. Pérez, L. R. Domingo, M. Duque-Noreña, E. Chamorro, *THEOCHEM* **2009**, *895*, 86–91.

[10] a) K. Watanabe, T. Mie, A. Ichihara, H. Oikawa, M. Honma, *J. Biol. Chem.* **2000**, *275*, 38393–38401; b) T. Ose, K. Watanabe, T. Mie, M. Honma, H. Watanabe, M. Yao, H. Oikawa, I. Tanaka, *Nature* **2003**, *422*, 185–189; c) C. R. W. Guimarães, M. Udier-Blagović, W. L. Jorgensen, *J. Am. Chem. Soc.* **2005**, *127*, 3577–3588.

[11] a) K. Afarinkia, V. Vinader, T. D. Nelson, G. H. Posner, *Tetrahedron* **1992**, *48*, 9111–9171; b) B. T. Woodard, G. H. Posner, *Advances in Cycloaddition* (Ed.: M. Harmata), JAI Press Inc, Greenwich, **1999**, p. 47–83; c) K. Kranjc, I. Leban, S. Polanc, M. Kočevar, *Heterocycles* **2002**, *58*, 183–189; d) K. Kranjc, S. Polanc, M. Kočevar, *Org. Lett.* **2003**, *5*, 2833–2836; e) K. Kranjc, M. Kočevar, F. Iosif, S. M. Coman, V. I. Parvulescu, E. Genin, J.-P. Genêt, V. Michelet, *Synlett* **2006**, 1075–1079; f) K. Kranjc, B. Štefane, S. Polanc, M. Kočevar, *J. Org. Chem.* **2004**, *69*, 3190–3193; g) K. Kranjc, M. Kočevar, *New J. Chem.* **2005**, *29*, 1027–1034; h) K. Kranjc, F. Perdih, M. Kočevar, *J. Org. Chem.* **2009**, *74*, 6303–6306.

[12] a) T. A. Bryson, D. M. Donelson, *J. Org. Chem.* **1977**, *42*, 2930–2931; b) P. Martin, J. Streith, G. Rihs, T. Winkler, D. Belluš, *Tetrahedron Lett.* **1985**, *26*, 3947–3950; c) P. Martin, E. Steiner, J. Streith, T. Winkler, D. Belluš, *Tetrahedron* **1985**, *41*, 4057–4078.

[13] R. E. Ireland, R. C. Anderson, R. Badoud, B. J. Fitzsimmons, G. J. McGarvey, S. Thaisrivongs, C. S. Wilox, *J. Am. Chem. Soc.* **1983**, *105*, 1988–2006.

[14] see the Supporting Information for details.

[15] C. Ester, A. Maderna, H. Pritzkow, W. Siebert, *Eur. J. Inorg. Chem.* **2000**, 1177–1184.

[16] a) C. Reichardt, *Solvents and Solvent Effect in Organic Chemistry*, Wiley-VHC, Weinheim, **2003**; b) R. Huisgen, *Pure Appl. Chem.* **1980**, *52*, 2283–2302.

[17] a) E. Gomez-Bengoa, M. D. Helm, A. Plant, J. P. A. Harrity, *J. Am. Chem. Soc.* **2007**, *129*, 2691–2699; b) D. L. Browne, J. F. Vivat, A. Plant, E. Gomez-Bengoa, J. P. A. Harrity, *J. Am. Chem. Soc.* **2009**, *131*, 7762–7769.

[18] G. Steiner, R. Huisgen, *Tetrahedron Lett.* **1973**, *14*, 3769–3776.

[19] a) K. Afarinkia, M. J. Bearpark, A. Ndibwami, *J. Org. Chem.* **2003**, *68*, 7158–7166; b) K. Afarinkia, M. J. Bearpark, A. Ndibwami, *J. Org. Chem.* **2005**, *70*, 1122–1133.

[20] a) A. D. Becke, *J. Chem. Phys.* **1993**, *98*, 5648–5652; b) C. Lee, W. Yang, R. G. Parr, *Phys. Rev. B* **1988**, *37*, 785–789.

[21] a) R. V. Stanton, K. M. Merz, *J. Chem. Phys.* **1994**, *100*, 434–443; b) J. Baker, M. Muir, J. Andzelm, *J. Chem. Phys.* **1995**, *102*, 2036–2079; c) B. Jursic, Z. Zdravkovski, *J. Chem. Soc. Perkin Trans. 2* **1995**, 1223–1226; d) E. Goldstein, B. Beno, K. N. Houk, *J. Am. Chem. Soc.* **1996**, *118*, 6036–6043; e) V. Branchadell, *Int. J. Quantum Chem.* **1997**, *61*, 381–388; f) A. Sbai, V. Branchadell, R. M. Ortuno, A. Oliva, *J. Org. Chem.* **1997**, *62*, 3049–3054; g) I. Morao, B. Lecea, F. P. Cossio, *J. Org. Chem.* **1997**, *62*, 7033–7036; h) L. F. Tietze, T. Pfeiffer, A. Schuffenhauer, *Eur. J. Org. Chem.* **1998**, 2733–2741; i) L. R. Domingo, M. Arno, J. Andres, *J. Am. Chem. Soc.* **1998**, *120*, 1617–1618; j) L. R. Domingo, M. J. Aurell, *J. Org. Chem.* **2002**, *67*, 959–965; k) L. R. Domingo, M. Arno, R. Contreras, P. Perez, *J. Phys. Chem. A* **2002**, *106*, 952–961; l) G. Orlova, J. D. Goddard, *J. Org. Chem.* **2001**, *66*, 4026–4035.

[22] W. J. Hehre, L. Radom, P. V. R Schleyer, J. A. Pople, *Ab initio Molecular Orbital Theory*, Wiley, New York, **1986**.

[23] *Gaussian 03*, Revision C.02, M. J. Frisch, G. W. Trucks, H. B. Schlegel, G. E. Scuseria, M. A. Robb, J. R. Cheeseman, J. A. Montgomery, T. Vreven Jr, K. N. Kudin, J. C. Burant, J. M. Millam, S. S. Iyengar, J. Tomasi, V. Barone, B. Mennucci, M. Cossi, G. Scalmani, N. Rega, G. A. Petersson, H. Nakatsuji, M. Hada, M. Ehara, K. Toyota, R. Fukuda, J. Hasegawa, M. Ishida, T. Nakajima, Y. Honda, O. Kitao, H. Nakai, M. Klene, X. Li, J. E. Knox, H. P. Hratchian, J. B. Cross, V. Bakken, C. Adamo, J. Jaramillo, R. Gomperts, R. E. Stratmann, O. Yazyev, A. J. Austin, R. Cammi, C. Pomelli, J. W. Ochterski, P. Y. Ayala, K. Morokuma, G. A. Voth, P. Salvador, J. J. Dannen-

 © 2010 Wiley-VCH Verlag GmbH & Co. KGaA, Weinheim

berg, V. G. Zakrzewski, S. Dapprich, A. D. Daniels, M. C. Strain, O. Farkas, D. K. Malick, A. D. Rabuck, K. Raghavachari, J. B. Foresman, J. V. Ortiz, Q. Cui, A. G. Baboul, S. Clifford, J. Cioslowski, B. B. Stefanov, G. Liu, A. Liashenko, P. Piskorz, I. Komaromi, R. L. Martin, D. J. Fox, T. Keith, M. A. Al-Laham, C. Y. Peng, A. Nanayakkara, M. Challacombe, P. M. W. Gill, B. Johnson, W. Chen, M. W. Wong, J. Gonzalez, A. C. Pople, Gaussian, Inc., Wallingford CT, **2004**.
[24] S. Miertus, E. Scrocco, J. Tomasi, *Chem. Phys.* **1981**, *55*, 117–129.
[25] M. Dai, D. Sarlah, M. Yu, S. J. Danishefsky, G. O. Jones, K. N. Houk, *J. Am. Chem. Soc.* **2007**, *129*, 645–657.
[26] P. Geerlings, F. De Proft, W. Langenaeker, *Chem. Rev.* **2003**, *103*, 1793–1873.
[27] C. Spino, H. Rezaei, Y. L. Dory, *J. Org. Chem.* **2004**, *69*, 757–764.
[28] a) A. Bongini, M. Panunzio, *Eur. J. Org. Chem.* **2006**, 972–977; b) A. Bongini, Z. Xia, M. Panunzio, *Eur. J. Org. Chem.* **2006**, 3533–3538.
[29] B. R. Ussing, C. Hang, D. A. Singleton, *J. Am. Chem. Soc.* **2006**, *128*, 7594–7607.
[30] B. K. Carpenter, *Angew. Chem. Int. Ed.* **1998**, *37*, 3340–3350.

Received: February 21, 2010
Published Online: August 31, 2010

 © 2010 Wiley-VCH Verlag GmbH & Co. KGaA, Weinheim